Original Research

A Novel MRI-Compatible Brain Ventricle Phantom for Validation of Segmentation and Volumetry Methods

Amanda F. Khan, MSc,[1,2] John J. Drozd, PhD,[2] Robert K. Moreland, MSc,[2,3] Robert M. Ta, MSc,[1,2] Michael J. Borrie, MB ChB,[3,4] Robert Bartha, PhD[1,2]* and the Alzheimer's Disease Neuroimaging Initiative

Purpose: To create a standardized, MRI-compatible, life-sized phantom of the brain ventricles to evaluate ventricle segmentation methods using T_1-weighted MRI. An objective phantom is needed to test the many different segmentation programs currently used to measure ventricle volumes in patients with Alzheimer's disease.

Materials and Methods: A ventricle model was constructed from polycarbonate using a digital mesh of the ventricles created from the 3 Tesla (T) MRI of a subject with Alzheimer's disease. The ventricle was placed in a brain mold and surrounded with material composed of 2% agar in water, 0.01% NaCl and 0.0375 mM gadopentetate dimeglumine to match the signal intensity properties of brain tissue in 3T T_1-weighted MRI. The 3T T_1-weighted images of the phantom were acquired and ventricle segmentation software was used to measure ventricle volume.

Results: The images acquired of the phantom successfully replicated in vivo signal intensity differences between the ventricle and surrounding tissue in T_1-weighted images and were robust to segmentation. The ventricle volume was quantified to 99% accuracy at 1-mm voxel size.

Conclusion: The phantom represents a simple, realistic and objective method to test the accuracy of lateral ventricle segmentation methods and we project it can be extended to other anatomical structures.

Key Words: 3T; brain phantom; MRI; ventricle; software validation; segmentation
J. Magn. Reson. Imaging 2012;36:476–482.

VOLUMETRY HAS DEMONSTRATED that large morphological changes occur in the brain during the course of Alzheimer's disease (AD) (1). In particular, enlargement of the lateral ventricles (cerebrospinal fluid-filled cavities in the interior of the cerebral hemispheres) has been consistently demonstrated and may be among the most sensitive of imaging biomarkers of AD progression (2). This enlargement is a consequence of the disease process; as surrounding healthy brain tissues atrophy, there is a corresponding increase in cerebrospinal fluid (CSF) within the ventricles. Currently, major efforts are under way to develop disease altering treatments for AD. The next generation of clinical trials for such compounds will benefit from objective methods, such as ventricle volumetry, to evaluate their effect on ventricular volume and potential disease modification. Volumetry may provide an outcome measure that could reliably distinguish between disease-modifying effects and purely symptomatic relief. Enlargement of the ventricles is also characteristic of other medical conditions such as schizophrenia, Parkinson's disease, hydrocephalus, and trauma to the brain (3–6). Ventricular measurement many be relevant to these conditions and related new treatment approaches as well.

Semiautomatic and fully automatic software has been developed to quantify ventricular volume, (along with other brain structures) using MRI scans acquired from patients with AD. Such programs include Freesurfer, Amira (Visage Imaging, Inc., San Diego, CA) and 3D Slicer (7,8). Measurement of ventricular volume is particularly amenable to segmentation due to the high signal intensity contrast between CSF and

[1]Medical Biophysics, Medical Sciences Building, The University of Western Ontario, London, ON, Canada.
[2]Robarts Research Institute, The University of Western Ontario, London, ON, Canada.
[3]Schulich School of Medicine and Dentistry, Clinical Skills Building, The University of Western Ontario, London, ON, Canada.
[4]Aging, Rehabilitation and Geriatric Care, Lawson Health Research Institute, London ON, Canada.

Data used in preparation of this article were obtained from the Alzheimer's Disease Neuroimaging Initiative (ADNI) database (adni.loni.ucla.edu). As such, the investigators within the ADNI contributed to the design and implementation of ADNI and/or provided data but did not participate in analysis or writing of this report. A complete listing of ADNI investigators can be found at: http://adni.loni.ucla.edu/wp-content/uploads/how_to_apply/ADNI_Authorship_List.pdf

Contract grant sponsor: National Institutes of Health; Contract grant numbers: U01 AG024904, P30 AG010129, K01 AG030514.

*Address reprint requests to: R.B., Imaging Research Laboratories, Robarts Research Institute, Schulich School of Medicine and Dentistry, The University of Western Ontario, 100 Perth Drive, London, ON, Canada N6A 5K8. E-mail: rob.bartha@robarts.ca

Received June 14, 2011; Accepted January 11, 2012.
DOI 10.1002/jmri.23612
View this article online at wileyonlinelibrary.com.

surrounding brain tissue in T_1-weighted MRI. When segmentation is performed in serial MRI scans of a patient, such quantification methods must be sensitive to very small volumetric changes in a complex 3D structure. However, absolute quantitative validation of image segmentation using in vivo data from patient scans is impossible because the exact volume of the lateral ventricles is unknown. To remedy this situation, a phantom can be used.

Physical phantoms are real models that can be imaged or simulated to test the performance of a segmentation method. One example of a physical ventricle phantom, by Chen et al (9), only modeled a single hemisphere of the brain and only half of the lateral ventricles (left ventricle). As well, their tissue mimicking solution did not match the T_1 relaxation time constants of brain tissue. In another example, Turkington et al (10) designed a 19-layer water-fillable cylinder phantom to mimic white matter, gray matter and ventricle perfusion rates, called the Hoffman phantom. However, because layers of their phantom were large (6.4-mm thick) compared with voxel resolution, their phantom had to be positioned so that layers of the phantom were parallel to transaxial slices to avoid discontinuities in edges. The Hoffman phantom also has not been used for ventricle segmentation and instead has been designed to test the registration of positron emission tomography (PET), single photon emission computed tomography (SPECT), and MRI images and activity distributions in PET (11). Digital phantoms are similar, except that a digital phantom is an image representation of a phantom that does not physically exist. Such phantoms are simulated MR images of the brain based on a series of registered MRI scans. Digital phantoms with simulated data, however, can suffer from an oversimplicity of phantom geometry, improper treatment of edge effects leading to tissue mixing in voxels and the improper modeling of the data acquisition method (12,13). Physical phantoms, on the other hand, are superior as they allow the fabrication of a controlled shape with known volume, from materials with predictable MRI properties. Physical phantoms are composed of synthetic materials that have a magnetic resonance signal that mimics that of human tissue and represent a completely objective measure to assess algorithm performance. It is important then, to validate the accuracy and precision of segmentation methods using a physical brain ventricle phantom of known volume that produces similar contrast to that observed in vivo.

A phantom to evaluate segmentation methods must: produce image signal intensities consistent with those observed in vivo, have homogenous relaxation times throughout, be life-size in scale and anatomically accurate in shape and proportions, and be straightforward and relatively inexpensive to fabricate. The phantom developed in the current study meets these criteria. It consists of a polycarbonate ventricle embedded in an agar mixture containing the paramagnetic compound, gadopentetate dimeglumine (Gd-DTPA), to modulate T_1 relaxation times to accurately simulate brain tissue, and sodium chloride (NaCl) to modulate conductivity.

The purpose of the current study was to construct a physical phantom that could be used as a gold standard to validate and compare different ventricle segmentation algorithms. Our phantom is the first physical phantom of the entire lateral ventricles for this purpose, known to the authors. The methodology described can also be extended to produce new physical phantoms that model other disease pathologies that present signal voids in MRI images.

MATERIALS AND METHODS

The phantom was constructed in two stages and consisted of a ventricle component and tissue model. The phantom was designed to accurately mimic the in vivo signal intensity difference between that of the ventricle and surrounding brain tissue. The signal intensity difference was chosen to be replicated because often it is this difference that segmentation algorithms rely on to identify ventricular voxels.

Ventricle Construction

Data used in the preparation of this article were obtained from the Alzheimer's Disease Neuroimaging Initiative (ADNI) database (adni.loni.ucla.edu). The ADNI was launched in 2003 by the National Institute on Aging (NIA), the National Institute of Biomedical Imaging and Bioengineering (NIBIB), the Food and Drug Administration (FDA), private pharmaceutical companies and nonprofit organizations, as a $60 million, 5-year public-private partnership. The primary goal of ADNI has been to test whether serial MRI, positron emission tomography (PET), other biological markers, and clinical and neuropsychological assessment can be combined to measure the progression of mild cognitive impairment (MCI) and early Alzheimer's disease.

A ventricle representing a typical subject with Alzheimer's disease was modeled by identifying an 80-year-old female representative subject (007_S_1339) from the ADNI database. This patient had a lateral ventricle volume of 48.8 cm^3 which was measured from their 1.5 Tesla (T) T_1-weighted MRI (processed with the ADNI GradWarp, B1 Correction, N3 Correction and scaling factor) using a previously reported ventricle volume measurement technique (2). This volume was chosen to be consistent with the average ventricle volume established for subjects with AD (49.9 ± 25.5 cm^3) (2). The subject's ADNI NIfTI image file was imported into ITK-SNAP (14), which is a free software application that can be used to segment anatomical structures in medical images. Using this program's semiautomatic level set segmentation algorithm, a rough digital wireframe mesh of the lateral ventricles was created. This was achieved by preprocessing the MRI scan with the image edges selection function and setting the scale of Gaussian blurring to 0.6 and the edge contrast value to 0.03 while keeping the standard edge mapping exponent at 2.0.

Preprocessing the image determines how intensity edges are utilized (i.e., by affecting the speed of snake propagation) when using the segmentation snake evolution algorithm that creates the mesh. Snake evolution is a method used by ITK-SNAP for segmentation of structures. "Snake" is used to refer to a closed curve that represents a segmented area. In snake evolution segmentation of the ventricle, the snake starts out as a "bubble point" (small circle segmentation) inside the ventricle structure and over time, it grows to fill the shape of the ventricle (15). To this end, bubble points were placed in the axial view, within the ventricle with varying radii under 2.0 mm to drive snake evolution. Many bubble points were placed to maximize regional growth while minimizing boundary leaking. The evolution of the snake ("snake evolution") is governed by a mathematical equation that describes the velocity of every point on the snake at any particular time. Snake evolution parameters such as balloon force and curvature force can be adjusted to limit voxel overgrowth. A manual hand contouring of the mesh using the deletion option of the paintbrush tool was then necessary to eliminate regions that had overgrown the anatomical boundaries of the ventricle by leaking to the surrounding white matter tracts or into the third ventricle. The refined mesh was then exported as a 3D STL file (a stereolithography CAD software format) and used to rapid prototype the ventricle from polycarbonate, using Fused Deposition Modelling by a Stratasys Vantage SE rapid prototyping machine (Stratasys Inc., 7665 Commerce Way, Eden Prairie, MN). The completed fabricated ventricle is shown in Figure 1a,b. The choice to fabricate the ventricle out of polycarbonate was made for two reasons: first, polycarbonate is a commonly used rapid prototyping material and second, this solid material has a very rapid T_2 relaxation rate, resulting in very little signal when scanned using typical echo-times (of greater than 3 ms), which is similar to the dark (low signal intensity) pixels produced by cerebrospinal fluid in T_1-weighted MRI scans.

Using the specific gravity of polycarbonate (1.2) and the weight of the fabricated ventricle, the final volume was determined to be 47.67 cm^3 ± 0.005 cm^3. The scale used to measure the fabricated ventricle was a Denver Instruments P-214 Precision Analytical Balance, which was internally calibrated using the DenverCal® precision internal weights. The specific gravity for the polycarbonate used is listed on the FORTUS 3D Production Systems Specification Sheet for Polycarbonate (www.stratasys.fr/download/MS-PC-FORTUS-0209.pdf). The volume of the ventricle was also determined a second way, using Archimedes' principle. An overflow can made of stainless steel was designed and the volume of the ventricle was equal to the volume of water displaced from the can into a beaker. With this measurement tool, the volume of the ventricle was determined to be 47.16 cm^3 ± 0.45 cm^3. It is important to note that the basic shape of the ventricle was defined using the original wire mesh model produced by ITK-SNAP. However, the production of the actual ventricle model involved several steps that may have resulted in slight alterations to the ventricle shape, including fused deposition modeling (with a machine accuracy of ± 0.127 mm or ± 0.0015 mm per mm, whichever is greater), sanding, and solvent sealing. For this reason, the final volume of the ventricle model was determined empirically, and was not estimated from the wire mesh model. Regarding anatomical boundaries of the ventricular system, the main body of the lateral ventricles are bordered by the corpus callosum, caudate nucleus, and thalamus. The left and right lateral ventricles are separated by the septum pellucidum and the fornix. The posterior portion of the lateral ventricle curves inferiorly into the occipital horn and the temporal horn. The temporal horn projects into the temporal lobe and is bounded by the hippocampus. The two lateral ventricles feed into the third ventricle through the interventricular foramen (16). In the current work, the third ventricle was not included in the model nor was the interventricular foramen. It should also be noted that the choroid plexus of each lateral ventricle, which is normally found in the central portion of the ventricle, with its intermediate intensity between CSF and white matter, may be a source of discrepancy between segmentation algorithms and was also not modeled.

Tissue Model

The second component of the phantom was the tissue-mimicking brain solution. To create this solution, the signal intensity of in vivo brain tissue needed to be accurately mimicked by the tissue model. The difference in signal intensity between the brain tissue and ventricle also needed to match in vivo results. To accomplish this goal, the signal intensity within tissue surrounding the lateral ventricles was measured in 3T T_1-weighted brain MRI images from 10 subjects with AD chosen at random from the ADNI database (17). Four regions of interest (ROI) were defined using ImageJ (18) in each dataset; two within the ventricle and the other two within the tissue surrounding the ventricle. From these four ROI locations, an average signal intensity (SI) difference of 261.5 ± 54.5 arbitrary units was calculated according to Eq. [1]:

$$\mathrm{SI} = \frac{SI_{\mathrm{ROI_1BrainTissue}} + SI_{\mathrm{ROI_2BrainTissue}}}{2} - \frac{SI_{\mathrm{ROI_1Ventricle}} + SI_{\mathrm{ROI_2Ventricle}}}{2} \quad [1]$$

The mixture surrounding the ventricles in the phantom was designed to replicate this signal intensity difference. Phantoms of 2% (w/v) agar dissolved in nanopure (distilled and deionized) water, 0.01% (w/v) NaCl and various molar concentrations of gadopentetate dimeglumine (Gd-DTPA) were created in 50-mL centrifuge tubes. First, the agar powder was dissolved in 50 mL of nanopure water at 55–60°C and heated until 85°C for 5 min on a combined hotplate/magnetic stirrer until the solution became clear (19–21). Following the addition of NaCl, Gd-DTPA (Magnevist®) was then added at concentrations ranging from 0 to 2.0 mM (v/v) per tube to alter T_1 relaxivity and stirred for one minute. The magnetic stir bar's usage was suspended

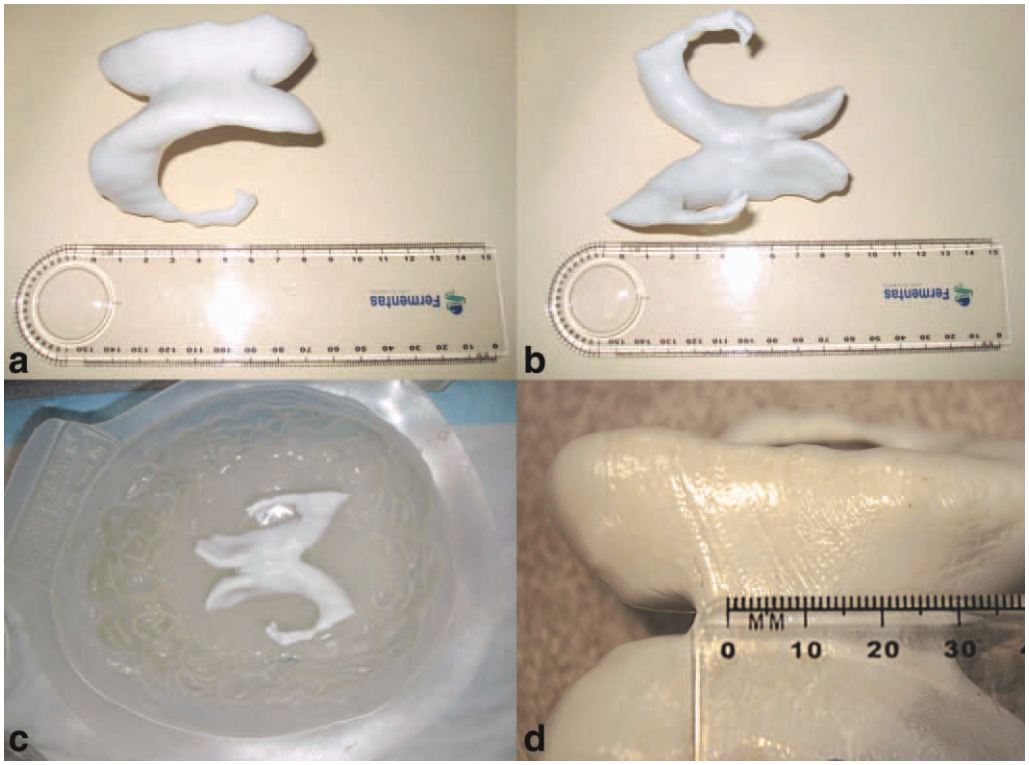

Figure 1. The construction of the brain ventricle phantom. **a,b:** The fabricated ventricle. **c:** Demonstrates the creation of a base for proper mid-brain positioning of the ventricle and Panel **d** is a close-up showing surface features.

for a period of 2 min to allow bubbles to rise to the surface and the solution was decanted into the centrifuge tube and allowed to cool to room temperature. Images of the tubes were acquired at 3T in a single session using the ADNI-specific 3D magnetization prepared rapid gradient-echo (MP-RAGE) sequence (2300/2.98 [TR/TE]; matrix, 256 × 240; flip angle, 9; field of view, 256 mm; slice thickness, 1.20 mm) on a Siemens Magnetom Tim Trio whole-body 3T MRI scanner with a 32 channel radiofrequency head coil (Siemens Healthcare, Erlangen, Germany). Signal intensities from each tube were measured and plotted against Gd-DTPA concentration.

Brain Ventricle Phantom

A life-size brain-shaped plastic mold (22,23) (SKS Sibley Co., El Segundo, CA) with the dimensions of 19 × 16 × 10 cm was used to contain the components of the brain phantom. The mold was first filled with 300 mL of tissue mimicking solution and allowed to cool to room temperature, to create a solid "base" for the fabricated ventricle to rest on so that the ventricle would be positioned within the brain mold at the proper mid-brain height (Fig. 1c). After, the ventricle was arranged in the middle of the brain on the base, 1400 mL of agar solution was poured in to fill the mold to the top. The completed brain ventricle phantom was allowed to rest undisturbed as it cooled so that all bubbles within the agar rose to the surface where they were skimmed off. The phantom was allowed to cool to room temperature overnight and then stored in a 4°C refrigerator. The phantom was then taken out of the refrigerator and allowed to warm to room temperature before imaging.

Validation of Ventricle Segmentation Software

The completed brain ventricle phantom was scanned on the same MRI scanner described above using the same ADNI-specific 3D MP-RAGE sequence used to scan the centrifuge phantom tubes. Images were acquired with an in-plane resolution of 1.0 mm^2, with slice thicknesses of 1.0, 1.5, 2.0, 3.0, 4.0, and 5.0 mm to determine the effect of slice thickness on quantification accuracy and precision. Images were analyzed using a fully automated segmentation tool in 3D Slicer developed in-house specifically for volumetric assessment of the lateral ventricles (8). The tool was developed using the Insight Segmentation and Registration Toolkit and the results were visualized in 3D Slicer. The program used selected seed points to initialize a confidence connected segmentation to generate a rough segmentation. A confidence connected segmentation chooses pixels whose intensities are within a multiple of standard deviations around a mean pixel intensity determined from seeds. The rough segmentation was enclosed in a bounding box and a fuzzy connectedness algorithm (24) was used to more accurately segment the ventricles within the bounding box. Fuzzy connectedness connects pixels based on an affinity function which incorporates intensities, gradients and distances between pixels. Affinities range between 0 and 1 and pixels are chosen based

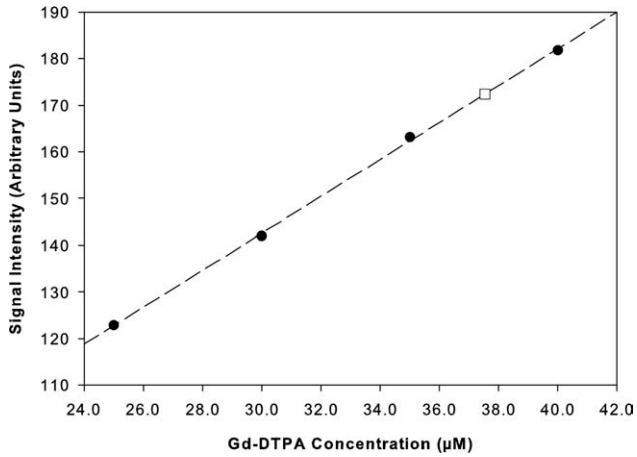

Figure 2. Gd-DTPA concentration plotted against signal intensity. The square point indicates the optimal concentration of Gd-DTPA, which was calculated to be 0.0375 mM.

on a threshold affinity. A second segmentation tool, using 3D Slicer's Editor Module, was also used to quantify the images (25). Grow Cut Segmentation was used to generate the initial label map. Then minimum and maximum pixel intensities were selected to perform Threshold Segmentation. 3D Slicer's "Save Island" feature was used to isolate the ventricle label map from the rest of the image and then the Label Statistics Module was used to count the number of pixels and calculate the volume of the ventricle label map.

RESULTS

The optimal concentration of Gd-DTPA to replicate the in vivo signal intensity difference between the lateral ventricles and surrounding tissue was determined to be 37.5 μM from the 50-mL centrifuge phantoms (Fig. 2). Representative T_1-weighted images of the completed brain ventricle phantom are shown in Figure 3a,b. The signal intensity difference between the ventricle and surrounding agar solution successfully matched in vivo signal intensity differences between the ventricle and surrounding brain tissue in 3T images from the ADNI database. The in vivo signal intensity difference was 261.5 ± 54.5 arbitrary units, whereas the signal intensity difference of the completed brain ventricle phantom was 262.9 ± 11.2 arbitrary units, which is a divergence of only 1.4 arbitrary units or 1%.

Figure 4 shows the quantified ventricle volume as a function of slice thickness using both our in-house segmentation program and 3D Slicer's Grow Cut algorithm. There was an overall trend that as voxel size increased, the accuracy of the ventricular volume calculation decreased. As well, as expected, due to partial volume effects, larger slice thicknesses resulted in an overestimation of the ventricle volume. At a resolution of 1.0 mm^3 isotropic, our in-house segmentation program reported a volume of 47.2 cm^3, whereas 3D Slicer's Grow Cut segmentation produced a volume of 47.13 cm^3, which is less than 1% smaller than the specific gravity derived volume of 47.67 cm^3 and less than 0.5% smaller than the volume derived with the overflow can measurements which was 47.16 cm^3. This result illustrates that our in-house software does a reasonable job of estimating ventricle volume under the conditions studied but further refinement may help improve the accuracy. For example, the use of the ventricle phantom allowed us to identify specific ventricular sub-regions where the volumetry algorithm initially failed. In particular, it has always been a challenge to delineate the temporal horn region. The phantom provided an opportunity to test and modify our fuzzy connectedness algorithm to optimize voxel classification in this area. This valuable information could not be reliably obtained by any other means. Figure 3c,d shows a 3D reconstruction of the ventricle segmentation performed at a slice thickness of 1.0 and 1.5 mm, respectively. From these images, specific points can be identified where the segmentation method failed, such as the thin connecting arms of the temporal horn.

DISCUSSION

A life-sized physical MRI-compatible brain ventricle phantom was successfully created using polycarbonate embedded in a tissue mimicking agar solution. This novel phantom was designed to emulate the appearance of the lateral brain ventricles in T_1-weighted MRI scans acquired at 3T using the ADNI MP-RAGE protocol. The cost of materials to fabricate the phantom was relatively inexpensive at approximately $400 CAD and in addition to refrigeration,

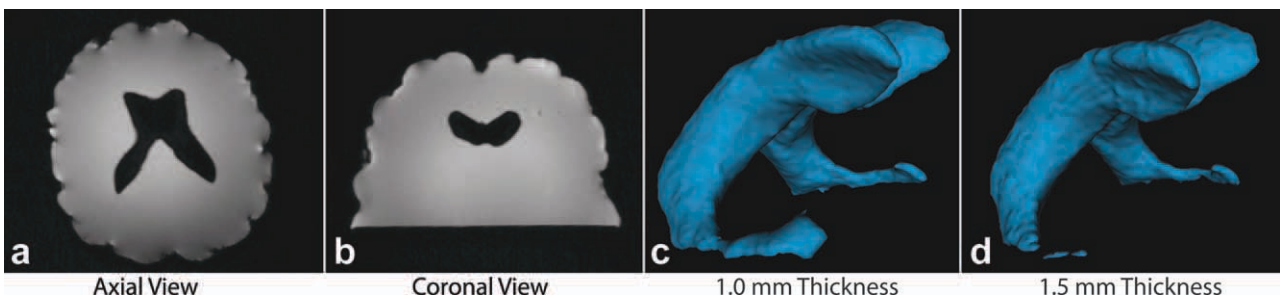

Figure 3. a,b: Axial and coronal slices, respectively of the MRI scan of the phantom at 3T. **c,d:** 3D reconstructions of the segmentation of the brain ventricle phantom at 1.0- and 1.5-mm slice thickness, respectively. [Color figure can be viewed in the online issue, which is available at wileyonlinelibrary.com.]

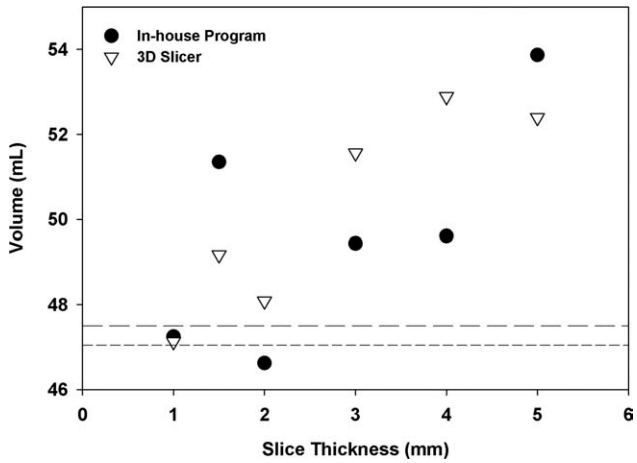

Figure 4. Segmented volumes plotted as a function of slice thickness. The circle data points were obtained using in-house segmentation software, while the upside down triangles were obtained with 3D Slicer's Grow Cut algorithm. The long dashed line represents the ventricle volume calculated using specific gravity and the short dashed line represents the volume calculated using Archimedes' principle.

preserving agents could be added to the agar solution to prolong the shelf life of the phantom. The overall creation was a simple process, and can be easily replicated by other groups to validate volumetry results using their segmentation methods. Images acquired for this study are freely available online, at http://www.robarts.ca/robert-bartha to any research groups wishing to use this data for software validation. Such images could provide a common, well-defined mechanism to compare the accuracy of different segmentation algorithms (26,27). As imaging markers such as ventricle expansion become established as indicators of disease progression and incorporated into clinical trials as surrogate endpoints, careful validation of segmentation methods must be performed to ensure the integrity of the study.

The methodology used to produce this phantom can also be applied to the simulation of any body tissue or structure that would appear dark in a T_1-weighted or T_2-weighted MRI scan. However, there are limitations to the use and generalizability of the current phantom. The ventricle model created in the current study represents an idealized ventricle shape. In vivo images of the ventricles may be complicated by additional factors not considered in the current work that could lead to additional sources of variability when making measurements of ventricle volume including the presence of blood vessels within the ventricle, the choroid plexus, intraventricular cysts, CSF flow artifacts, periventricular signal variation bordering the ventricles, and the presence of the interventricular foramen and the third ventricle. It is also not possible to segment the phantom with some segmentation software tools such as Freesurfer because the Freesurfer pipeline uses a large amount of neuroanatomical information and our phantom does not include all parts of the brain. These limitations of the phantom's design could be remedied in future incarnations. Subsequent phantoms will be more complex and will include additional modeling of the anterior and posterior commissure white matter tracts, the corpus callosum and the third and fourth ventricles.

In conclusion, the phantom produced in the current study effectively simulated the appearance and shape of the lateral ventricles of the brain and successfully mimicked the signal intensity properties of both ventricle and surrounding tissue in T_1-weighted MRI scans. Such phantoms should be used as gold standards in the validation of ventricle segmentation software algorithms.

ACKNOWLEDGMENTS

The authors thank Chris Vandelaar of University Machine Services for his respected input regarding the fabrication of the ventricle, Lauren Villemaire for her helpful guidance in respect to the agar tissue model; Dr. Stephen Pasternak for the brain mold and use of laboratory equipment; Dr. Ravi Menon for laboratory supplies; Joe Gati for his feedback about image processing, Kim Krueger and Adam McLean for their valued assistance in scanning, Kevin Barker for the construction of the overflow can, Mark Froncisz for his photography skills and Michal Marynowski for his overall support. Data collection and sharing for this project was funded by the Alzheimer's Disease Neuroimaging Initiative (ADNI). ADNI is funded by the National Institute on Aging, the National Institute of Biomedical Imaging and Bioengineering, and through generous contributions from the following: Abbott, AstraZeneca AB, Bayer Schering Pharma AG, Bristol-Myers Squibb, Eisai Global Clinical Development, Elan Corporation, Genentech, GE Healthcare, GlaxoSmithKline, Innogenetics, Johnson and Johnson, Eli Lilly and Co., Medpace, Inc., Merck and Co., Inc., Novartis AG, Pfizer Inc, F. Hoffman-La Roche, Schering-Plough, Synarc, Inc., as well as nonprofit partners the Alzheimer's Association and Alzheimer's Drug Discovery Foundation, with participation from the U.S. Food and Drug Administration. Private sector contributions to ADNI are facilitated by the Foundation for the National Institutes of Health (www.fnih.org). The grantee organization is the Northern California Institute for Research and Education, and the study is coordinated by the Alzheimer's Disease Cooperative Study at the University of California, San Diego. ADNI data are disseminated by the Laboratory for Neuro Imaging at the University of California, Los Angeles. Ontario Graduate Scholarship in Science and Technology, Ontario Research Fund: Building a Better Brain, National Institutes of Health.

REFERENCES

1. Schott JM, Price SL, Frost C, Whitwell JL, Rossor MN, Fox NC. Measuring atrophy in Alzheimer disease: a serial MRI study over 6 and 12 months. Neurology 2005;65:119–124.
2. Nestor SM, Rupsingh R, Borrie M, et al. Ventricular enlargement as a possible measure of Alzheimer's disease progression validated using the Alzheimer's disease neuroimaging initiative database. Brain 2008;131(Pt 9):2443–2454.
3. Poca MA, Sahuquillo J, Mataro M, Benejam B, Arikan F, Baguena M. Ventricular enlargement after moderate or severe head injury:

a frequent and neglected problem. J Neurotrauma 2005;22: 1303–1310.
4. Apostolova LG, Beyer M, Green AE, et al. Hippocampal, caudate, and ventricular changes in Parkinson's disease with and without dementia. Mov Disord 2010;25:687–688.
5. Kempton MJ, Stahl D, Williams SC, DeLisi LE. Progressive lateral ventricular enlargement in schizophrenia: a meta-analysis of longitudinal MRI studies. Schizophr Res 2010;120:54–62.
6. Del Bigio MR. Neuropathology and structural changes in hydrocephalus. Dev Disabil Res Rev 2010;16:16–22.
7. Fischl B, Salat DH, Busa E, et al. Whole brain segmentation: automated labeling of neuroanatomical structures in the human brain. Neuron 2002;33:341–355.
8. Pieper S, Lorensen B, Schroeder W, Kikinis R. The NA-MIC Kit: ITK, VTK, Pipelines, Grids and 3D Slicer as an Open Platform for the Medical Image Computing Community. Proc IEEE Intl Symp Biomed Imaging ISBI 2006:698–701.
9. Chen SJ, Hellier P, Gauvrit JY, Marchal M, Morandi X, Collins DL. An anthropomorphic polyvinyl alcohol triple-modality brain phantom based on Colin27. Med Image Comput Comput Assist Interv 2010;13(Pt 2):92–100.
10. Turkington TG, Jaszczak RJ, Pelizzari CA, et al. Accuracy of registration of PET, SPECT and MR images of a brain phantom. J Nucl Med 1993;34:1587–1594.
11. Hoffman EJ, Cutler PD, Digby WM, Mazziotta JC. 3-D phantom to simulate cerebral blood flow and metabolic images for PET. IEE Trans Nucl Sci 1990;37:616–620.
12. Collins DL, Zijdenbos AP, Kollokian V, et al. Design and construction of a realistic digital brain phantom. IEEE Trans Med Imaging 1998;17:463–468.
13. Alfano B, Comerci M, Larobina M, et al. An MRI digital brain phantom for validation of segmentation methods. Med Image Anal 2011;15:329–339.
14. Yushkevich PA, Piven J, Hazlett HC, et al. User-guided 3D active contour segmentation of anatomical structures: significantly improved efficiency and reliability. Neuroimage 2006;31:1116–1128.
15. Yushkevich PA, Zhang H, Goodlett C, Burke T, Tustison N. ITK-SNAP: Section 5, Introduction to Automatic Segmentation. ITK-SNAP Tutorial; 2009. Available at: http://www.itksnap.org/pmwiki/pmwiki.php?n=Documentation.TutorialSectionIntroduc tionToAutomatic.
16. O'Rahilly R. Basic Human Anatomy. Dartmouth Medical School 2008. Available at: http://www.dartmouth.edu/~ humananatomy/.
17. Mueller SG, Weiner MW, Thal LJ, et al. The Alzheimer's disease neuroimaging initiative. Neuroimaging Clin N Am 2005;15: 869–877, xi–xii.
18. Abramoff MD, Magelhaes PJ, Ram SJ. Image processing with ImageJ. Biophotonics Int 2004;11:36–42.
19. Kraft KA, Fatouros PP, Clarke GD, Kishore PR. An MRI phantom material for quantitative relaxometry. Magn Reson Med 1987;5:555–562.
20. Kato H, Kuroda M, Yoshimura K, et al. Composition of MRI phantom equivalent to human tissues. Med Phys 2005;32:3199–3208.
21. Gilbert KM, Curtis AT, Gati JS, Klassen LM, Villemaire LE, Menon RS. Transmit/receive radiofrequency coil with individually shielded elements. Magn Reson Med 2010;64:1640–1651.
22. Field AS, Yen YF, Burdette JH, Elster AD. False cerebral activation on BOLD functional MR images: study of low-amplitude motion weakly correlated to stimulus. AJNR Am J Neuroradiol 2000;21:1388–1396.
23. Reinertsen I, Collins DL. A realistic phantom for brain-shift simulations. Med Phys 2006;33:3234–3240.
24. Saha PK, Udupa JK. Fuzzy connected object delineation: axiomatic path strength definition and the case of multiple seeds. Comput Vis Image Underst 2001;83:275–295.
25. Gering DT, Nabavi A, Kikinis R, et al. An integrated visualization system for surgical planning and guidance using image fusion and an open MR. J Magn Reson Imaging 2001;13:967–975.
26. Barra V, Frenoux E, Boire JY. Automatic volumetric measurement of lateral ventricles on magnetic resonance images with correction of partial volume effects. J Magn Reson Imaging 2002;15:16–22.
27. Kovacevic S, Rafii MS, Brewer JB. High-throughput, fully automated volumetry for prediction of MMSE and CDR decline in mild cognitive impairment. Alzheimer Dis Assoc Disord 2009;23:139–145.